Polymer Bulletin 10, 547–552 (1983)

Polymer Bulletin

Melt-Crystallization of *n*-Alkanes and Polyethylene in a Temperature Gradient

1. Crystalline Orientation of Grown Specimens

Tsutomu Asano

Department of Physics, Faculty of Science, Shizuoka University, Shizuoka, 422, Japan

Summary

Normal alkanes and polyethylene were crystallized from a melt state in a temperature gradient. The feature of the crystallization depends both on the crystallizing speed and on the tube diameter of the specimen. Crystalline orientations of the grown specimens, investigated by X-ray diffraction method, are possible to classify into two orientations: One is that the c*-axis is perpendicular to the growth direction, and the other parallel to it.

Introduction

Crystalline structures of normal alkanes (C_nH_{2n+2}) are known to exhibit a polymorphism depending both on the number and on the parity of n. When n is odd, the stable crystalline form is orthorhombic. When n is even, the crystalline form is classified into the three systems; triclinic ($n \leq 26$) and monoclinic or, if the material is not quite pure, orthorhombic ($26 \leq n \leq 36$) (BROADHURST 1962). Almost all structural studies of n-alkanes have been carried out by specimens consist of solution grown single crystals. In order to examine melt-crystallization, n-alkanes and polyethylene were crystallized in a temperature gradient. The feature of the crystallization at the solid-melt interfacial plane was observed by the polarization microscopy. The crystalline orientation of the grown specimen was measured by X-ray diffraction method after crystallization.

Experimental

1) Materials used.
Specimens of n-alkanes used are eicosane ($C_{20}H_{42}$), heneicosane ($C_{21}H_{44}$), docosane ($C_{22}H_{46}$), tricosane ($C_{23}H_{48}$), tetracosane ($C_{24}H_{50}$), pentacosane ($C_{25}H_{52}$), hexacosane ($C_{26}H_{54}$), heptacosane ($C_{27}H_{56}$), octacosane ($C_{28}H_{58}$), nonacosane ($C_{29}H_{60}$) and hexatriacontane ($C_{36}H_{74}$) of WAKO Pure Chemical Industries Co. Ltd., whose purities are better than 95 %. (These are hereinafter abbreviated to C20, C21, C22, C23 C24, C25, C26, C27, C28, C29 and C36.) Specimens of polyethylene used are fractionated PE 1000 and PE 2000 of Polymer Laboratories Ltd., and NBS 1484 linear polyethylene (M_W = 119,600 M_W/M_N = 1.19). PE 1000 and PE 2000 correspond to n-alkanes of C71 and C143, respectively.

2) Crystallization apparatus.
Fig.1 shows a schematic view of the crystallization apparatus. Temperature gradient was set up between a cylindrical heater and a cooler. We define z-axis along the center axis of the heater and cooler. Temperature of the heater was controlled by a thermistor regulator at a temperature higher than the melting point of the specimen. The cooler was constantly cooled by water to 20 °C. The spacing between the heater and the cooler was 2 mm. The steep temperature gradient was produced in the gap, which was varied depending on the temperature of the heater. For instance, it was kept about 70 °C/mm for polyethylene, about 30 °C/mm for C36 and about 20 °C/mm for C21.

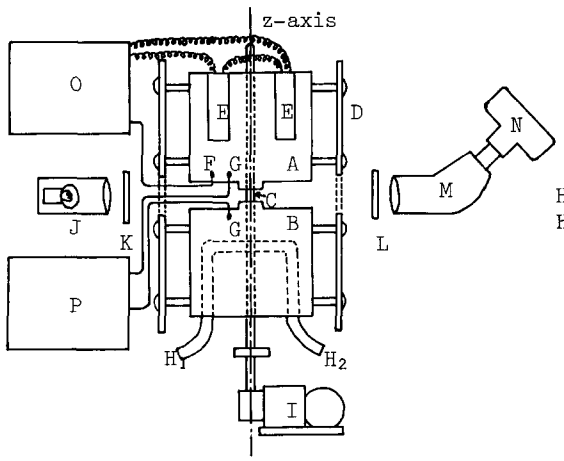

A: heater
B: cooler
C: sample tube
D: holder
E: nichrome heater
F: thermistor
G: thermo-couple
H_1: water inlet
H_2: water outlet
I: sample carrier
J: light source
K: polarizer
L: analyzer
M: microscope
N: camera
O: temp. controller
P: recorder

Fig.1 Schematic view of a crystallization apparatus

A sample was vacuum-sealed in a 0.1 mm thick glass tube, whose outer diameter R was ranged in 0.5 mm, 1.0 mm, 1.5 mm and 2.0 mm. When the sample tube was placed in a temperature gradient, the solid-melt interfacial plane appeared between the heater and the cooler. The crystallization proceeded only when the sample was moved from the heater to the cooler along the z-axis by a sample carrier. The velocities of the sample carrier (V) were 2 mm/hr, 6 mm/hr, 18 mm/hr, 2 mm/min, 6 mm/min and 18 mm/min. The crystallizing plane was observed by a polarization microscope with crossed polaroids. The feature of the crystallization was recorded by a camera. After crystallization was carried out, the sample was removed from the apparatus and X-ray diffraction scattering measurement was done at the room temperature.

Results

1) Polarization Microscopy.
In the course of crystallization, solid-melt boundary plane shows different appearances depending both on the crystallizing speed and on the diameter of the sample tube. When the sample tube is begun to move with a speed faster than 2 mm/min, the boundary plane moves downwards to the cooler and the crystalline surface becomes very rough consisting of needle-like crystals for all the tube

diameters. In the cases of 2 mm/hr, 6 mm/hr and 18 mm/hr, the boundary plane is smooth and three types of movement of growing planes are observed:
a) It moves downwards by about 100~200μ, and apparent supercooling zone is recognized. This type of crystallization appears in PE, PE 2000 and PE 1000 for all the tube diameters.
b) It moves downwards at the first stage of the crystallization for about 5 min. Thereafter it moves upwards and after 30 min it lies upper than the position before the start of moving by about 100~200 μ. This upper crystallizing plane is stable and successive crystallization steadily proceeds at this plane. After the motion is stopped, the boundary plane does not move even more than one hour. This type clearly appears on even number alkanes of $24 \leq n \leq 36$ when V=2 mm/hr.
c) It hardly changes during the crystallization from the initial position before the crystallization. This type is observed in C20, C22 and odd number n-alkanes for all the tube diameters.

2) X-ray Diffraction Measurements.
The grown specimen was studied by WAXS and SAXS at the room temperature. The crystalline orientation was analyzed mainly by the orientation of 110, 100 (or 200), 010 (or 020) and 001 (or 002, 003, ...) reflections. In the case of n-alkanes, the direction of the c*-axis (the normal of the (00ℓ) planes) is easily observed because the 00ℓ reflections are aligned in the X-ray patterns. The degree of orientation was measured by the arc stretch of these reflections. The results when R=1.5 mm are summarized in the TABLE.

The crystalline orientation is greatly affected by crystallizing speed. When V is faster than 6 mm/min, no orientation is observed. Only slight orientation appears when V=2 mm/min. In general, degree of orientation is best when V=2 mm/hr, though there are several exceptions.
The effect of the tube diameter on the orientation is clear in PE. The orientation is very sharp when R=0.5 mm, but it becomes broad when R=1.0 mm and no orientation can no longer be observed when R=1.5 and R=2.0 mm. PE 2000 and PE 1000 show that the degree of orientation is best when R=1.0 mm. On the other hand, n-alkanes show poor orientation when R=0.5 mm. The best orientation of them appears when R=1.5 mm, but the degree of orientation is greatly different depending on n.

For the diameter of 1.5 mm, the WAXS patterns of C20 and C22 show that the c*-axis is perpendicular to the z-axis ($c^* \perp z$). The triclinic b-axis is parallel to the z-axis in C20 whereas the a-axis is parallel to it in C22. WAXS patterns of the odd number n-alkanes show that the c*-axis is perpendicular to the z-axis where the orthorhombic a- and b-axes are also rotated around the c*-axis. The WAXS pattern of C24 at the crystallization speed of 2 mm/hr shows that the c*-axis is parallel to the z-axis ($c^* // z$). The same orientation is observed in C26, C28 and C36. This type of orientation arises only when the upper crystallizing plane appears in the polarization microscopy.
For the diameter of 0.5 mm, the SAXS patterns of PE, PE 2000 and PE 1000 show that the normal of the crystalline layer is perpendicular to the z-axis. The long spacings of PE 2000 and PE 1000 are

TABLE

Crystalline orientation (O) and degree of orientation (D) of n-alkanes and polyethylenes when R=1.5 mm.

Crystallizing Speed		18 mm/hr	6 mm/hr	2 mm/hr
C20 (tricli.)	O	c*⊥z (b// z)	c*⊥z (b// z)	c*⊥z (b// z)
	D	+	++	++
C21 (ortho.)	O	c*⊥z	c*⊥z	c*⊥z
	D	+	++	++
C22 (tricli.)	O	c*⊥z (a// z)	c*⊥z (a// z)	c*⊥z (a// z)
	D	+	+++	+++
C23 (ortho.)	O	c*⊥z	c*⊥z	c*⊥z
	D	+	++	+
C24 (tricli./monocli.)	O	c*⊥z (a// z)	c*⊥z (a// z)	c*// z
	D	+	++	++
C25 (ortho.)	O	c*⊥z	c*⊥z	
	D	+	+	-
C26 (monocli.)	O		c*⊥z (a// z)	c*// z
	D	-	+	++
C27 (ortho.)	O		c*⊥z	c*⊥z
	D	-	+	+
C28 (monocli.)	O	c*// z	c*// z	c*// z
	D	++	+	+
C29 (ortho.)	O	c*⊥z	c*⊥z	
	D	+	+	-
C36 (ortho./monocli.)	O		c*// z	c*// z
	D	-	+	++
PE 1000 (ortho.)	O	c*⊥z (b// z)	c*⊥z (b// z)	c*⊥z (b// z)
	D	++	++	++
PE 2000 (ortho.)	O	c*⊥z (b// z)	c*⊥z (b// z)	c*⊥z (b// z)
	D	++	+++	+++
PE (NBS) (ortho.)	O			
	D	-	-	-

c*// z means that the c*-axis is parallel to the z-axis.
c*⊥z means that the c*-axis is perpendicular to the z-axis.
- ; The WAXS pattern shows a uniform ring and no crystalline orientation is observed.
+ ; The WAXS pattern shows that the stretch of an arc is ca.±50° from the center of the arc. The degree of orientation is low.
++ ; The WAXS pattern shows that the stretch of an arc is ca. ±20° from the center of the arc. The degree of orientation is intermediate.
+++ ; The WAXS pattern shows that the stretch of an arc is less than ±10°. The degree of orientation is high.

175 Å and 95 Å, respectively, which well coincide with the molecular lengths of 180 Å and 90 Å. The WAXS patterns of these samples show that the orthorhombic b-axis is parallel to the z-axis.

Discussion

As shown in Fig.2, the four typical orientations are investigated in the melt-crystallized specimen:

1) The c*-axis is perpendicular and the a-axis is parallel to the z-axis, which is observed in C22, C24 and C26.
2) The c*-axis is perpendicular and the b-axis is parallel to the z-axis, which is observed in C20, PE 1000, PE 2000 and PE.
3) The c*-axis is perpendicular to the z-axis, and both the a- and b-axes are rotated around the c*-axis, which is observed in C21, C23, C25, C27 and C29.
4) The c*-axis is parallel to the z-axis, which is observed in C24, C26, C28 and C36.

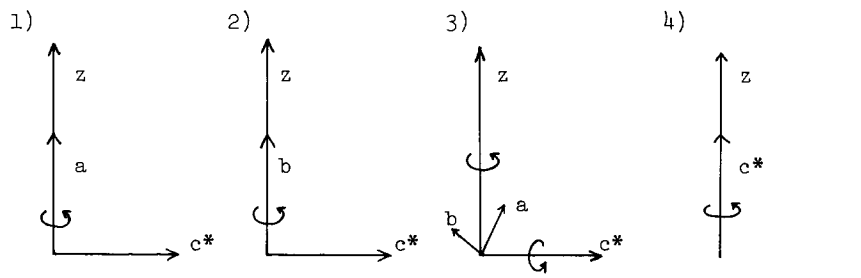

C22, C24, C26	C20, PE 1000, PE 2000, PE	C21, C23, C25, C27, C29	C24, C26, C28, C36

Fig.2 Four typical orientations of melt-grown specimens

It is possible to classify the orientations of melt-crystallized materials into the c*⊥ z orientation (1~3) and the c*// z orientation (4). The c*// z orientation is deeply related to the upper crystallizing plane appearing in the polarization microscopy. In C24 and C26, the c*⊥ z orientation at 18 mm/hr and at 6 mm/hr changes to the c*// z orientation at 2 mm/hr, which corresponds to the appearance of the upper crystallizing plane at 2 mm/hr.

In the case of solution grown single crystals, the spiral growth mechanism has been frequently observed. Especially in even number n-alkanes, the polytypism and polysynthetic twins caused by the nucleation of the spiral growth have been reported (BOISTELLE et al. 1976, AQUILANO 1977, RINAUDO et al. 1981). In the case of melt-crystallization, the similar crystallizing mechanism seems to occur in several even number n-alkanes.

As shown in Fig.3, G_1 and G_2 are the growth rates in the direction of intralayer and that of interlayer, respectively. Usually $G_1 > G_2$, because it is easier to adhere the molecular chain into the layer than to form a nucleus on the layer. However, the energy for the nucleation is much reduced by the screw dislocation. Accordingly, G_2 exceeds G_1 when screw dislocation arises on the crystallizing plane. Then, the crystallization easily proceeds along G_2, and the apparent supercooling decreases. As a result, the upper crystallizing plane appears and the orientation of the c*-axis is parallel to the crystallizing direction (c*// z).

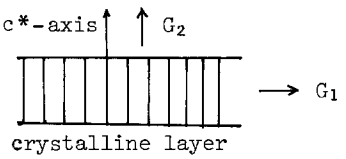

Fig.3

Acknowledgements

The author would like to acknowledge Prof. Y. Fujiwara of Shizuoka Univ. for valuable discussions throughout the experiment, and Asst. Prof. T. Yoshida for reading the manuscript. Thanks are also to M. Fukazu, N. Ishikawa and Y. Ito for assistance of the experiment.

References.

AQUILANO, D.: J. Crystal Growth 37, 215 (1977)
BOISTELLE, R., SIMON, B. and PÈPE, G.: Acta Cryst. B32. 1240 (1976)
BROADHURST, M. G.: J. Res. Natl. Bur. Stand. 66A, 241 (1962)
RINAUDO, C., AQUILANO, D and ABBONA, F.: J. Crystal Growth 53, 361 (1981)

Accepted August 31, 1983